Biochemical Pharmacology 89 (2014) 321–328

Contents lists available at ScienceDirect

Biochemical Pharmacology

journal homepage: www.elsevier.com/locate/biochempharm

Inhibition of RND-type efflux pumps confers the FtsZ-directed prodrug TXY436 with activity against Gram-negative bacteria

Malvika Kaul [a], Yongzheng Zhang [b], Ajit K. Parhi [b], Edmond J. LaVoie [c], Daniel S. Pilch [a,*]

[a] Department of Pharmacology, Rutgers Robert Wood Johnson Medical School, Piscataway, NJ 08854-5635, United States
[b] Taxis Pharmaceuticals, Inc., North Brunswick, NJ 08902, United States
[c] Department of Medicinal Chemistry, Ernest Mario School of Pharmacy, Rutgers-The State University of New Jersey, Piscataway, NJ 08855, United States

ARTICLE INFO

Article history:
Received 17 December 2013
Accepted 7 March 2014
Available online 14 March 2014

ABSTRACT

Infections caused by Gram-negative bacterial pathogens are often difficult to treat, with the emergence of multidrug-resistant strains further restricting clinical treatment options. As a result, there is an acute need for the development of new therapeutic agents active against Gram-negative bacteria. The bacterial protein FtsZ has recently been demonstrated to be a viable antibacterial target for treating infections caused by the Gram-positive bacteria *Staphylococcus aureus* in mouse model systems. Here, we investigate whether an FtsZ-directed prodrug (TXY436) that is effective against *S. aureus* can also target Gram-negative bacteria, such as *Escherichia coli*. We find that the conversion product of TXY436 (PC190723) can bind *E. coli* FtsZ and inhibit its polymerization/bundling *in vitro*. However, PC190723 is intrinsically inactive against wild-type *E. coli*, with this inactivity being derived from the actions of the efflux pump AcrAB. Mutations in *E. coli* AcrAB render the mutant bacteria susceptible to TXY436. We further show that chemical inhibition of AcrAB in *E. coli*, as well as its homologs in *Klebsiella pneumoniae* and *Acinetobacter baumannii*, confers all three Gram-negative pathogens with susceptibility to TXY436. We demonstrate that the activity of TXY436 against *E. coli* and *K. pneumoniae* is bactericidal in nature. Evidence for FtsZ-targeting and inhibition of cell division in Gram-negative bacteria by TXY436 is provided by the induction of a characteristic filamentous morphology when the efflux pump has been inhibited as well as by the lack of functional Z-rings upon TXY436 treatment.

1. Introduction

FtsZ is an essential protein for bacterial cell division (cytokinesis) and viability [1–3]. It self-polymerizes in a GTP-dependent manner to form a ring-like structure (the Z-ring) at the bacterial midcell [4–6]. This structure becomes anchored to the bacterial membrane, and acts as a scaffold for the recruitment of other cell division proteins and thus formation of the mature divisome [7–9]. Because of its essential nature, FtsZ is an attractive new target for antibiotic development that is not exploited by any current clinical agent [10–24].

The benzamide derivative PC190723 (Fig. 1) was one of the first FtsZ-targeting antibacterial agents to be identified [13]. While exhibiting potent activity against a number of Gram-positive bacteria (including staphylococci and bacilli), PC190723 has been shown to be associated with poor activity against Gram-negative species [10,12,13,23,25]. It has been suggested that the poor activity of PC190723 against the Gram-negative pathogen *Escherichia coli* may reflect a corresponding inability to target *E. coli* FtsZ effectively [26].

The studies described herein are aimed at furthering our understanding of the basis for the poor activity of PC190723 against Gram-negative bacteria. We elected to use a prodrug of PC190723 (TXY436; see structure in Fig. 1) in these studies, since PC190723 itself is associated with poor formulation properties and limited antibacterial efficacy *in vivo* [27]. At physiological pH, TXY436 converts to PC190723 within minutes, while also exhibiting significant oral and intravenous efficacy *in vivo* against systemic infection with both the methicillin-sensitive and methicillin-resistant forms of the Gram-positive pathogen *Staphylococcus aureus* [27]. In the present studies, we evaluate the impact of TXY436 on FtsZ function, morphology, and viability of various Gram-negative bacteria. We show that TXY436 is inactive against wild-type strains of *E. coli*, *Klebsiella pneumoniae*, and *Acinetobacter baumannii*. However, in *E. coli*, this inactivity is due to the actions of the *r*esistance-*n*odulation-cell *d*ivision (RND)-type

* Corresponding author.
E-mail address: pilchds@rwjms.rutgers.edu (D.S. Pilch).

http://dx.doi.org/10.1016/j.bcp.2014.03.002
0006-2952/

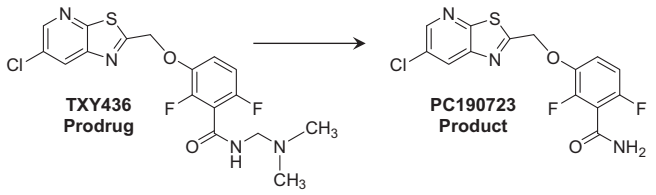

Fig. 1. Structures of the TXY436 prodrug and its conversion product PC190723.

efflux pump AcrAB, and does not reflect an inability on the part of TXY436 to target FtsZ function and disrupt cell division. We also show that RND efflux pump inhibition renders TXY436 active against not only *E. coli*, but also against *K. pneumoniae* and *A. baumannii*. These collective findings provide insights into potential strategies for targeting Gram-negative bacteria with FtsZ-directed compounds related to TXY436 that include co-treatment with RND efflux pump inhibitors (EPIs).

2. Materials and methods

2.1. Bacterial strains, FtsZ proteins, TXY436, antibiotics, chemicals, and solvents

E. coli W4573, N43 (*acrA1*), LZ2301 (*ΔmdfA*), LZ2096 (*ΔnorE*), and LZ2310 (*acrA1 ΔmdfA ΔnorE*) were gifts from Dr. Lynn Zechiedrich (Baylor College of Medicine, Houston, TX) [28]. *E. coli* KG22-pLAU80 was a gift from Dr. Liam Good (Royal Veterinary College, University of London, England) [29]. All other *E. coli*, *K. pneumoniae*, and *A. baumannii* strains were obtained from the American Type Culture Collection (ATCC, Manassas, VA). Purified *E. coli* FtsZ was obtained from Cytoskeleton, Inc. (Denver, CO). *S. aureus* FtsZ was expressed in *E. coli* and purified as described previously [17]. TXY436 and PC190723 were synthesized as previously described in [27] and [30], respectively. Phenylalanine-arginine-β-naphthylamide 2HCl (PAβN), minocycline HCl, and ampicillin were obtained from Sigma-Aldrich Co. (St. Louis, MO), as were all other reagents and solvents, unless otherwise indicated.

2.2. Fluorescence anisotropy assay

All steady-state fluorescence anisotropy experiments were conducted at 25 °C on an AVIV Model ATF105 Spectrofluorometer (Aviv Biomedical, Lakewood, NJ) equipped with a thermoelectrically controlled cell holder and computer-controlled Glan–Thompson polarizers in both the excitation and emission directions. 1 μM of a non-hydrolyzable GTP analog (GTPγS) conjugated to the fluorescent dye BODIPY (BoGTPγS; obtained from Life Technologies Corp. [Grand Island, NY] as the sodium salt in a 5 mM stock solution) was combined with 5 μM *E. coli* or *S. aureus* FtsZ and either PC190723 or GTP (Roche Diagnostics GmbH, Mannheim, Germany), at concentrations ranging from 0 to 240 μM, in 150 μL of solution containing 50 mM Tris-HCl (pH 7.4), 50 mM KCl, and 2 mM magnesium acetate. After incubation for 5 min at 25 °C, the fluorescence emission intensities (I) of BoGTPγS were measured with the excitation polarizer oriented vertically and the emission polarizer oriented vertically (I_{VV}) or horizontally (I_{VH}). BoGTPγS anisotropy (r) values were then determined using the following relationship:

$$r = \frac{I_{VV} - GI_{VH}}{I_{VV} + 2GI_{VH}} \quad (1)$$

G represents the instrument correction factor, and is given by the ratio of the fluorescence emission intensity acquired with the excitation polarizer oriented horizontally and the emission polarizer oriented vertically (I_{HV}) to that acquired with both the excitation and emission polarizers oriented horizontally (I_{HH}). A G value was measured at the start of each acquisition. The slit widths were set at 4 nm in both the excitation and emission directions, with the excitation and emission wavelengths being set at 488 and 510 nm, respectively. A quartz ultra-micro cell (Hellma USA, Inc., Plainview, NY) with a 2 × 5 mm aperture and a 15 mm center height was used for all measurements. The pathlengths in the excitation and emissions directions were 1 and 0.2 cm, respectively. All anisotropy experiments were conducted in triplicate, with the reported anisotropies reflecting the average values.

BoGTPγS anisotropy profiles acquired as a function of PC190723 or GTP concentration were analyzed with the following 1:1 binding formalism to yield compound-protein dissociation constants (K_d):

$$r = r_0 + \frac{r_\infty - r_0}{2[P]_{tot}} \times \left[\left([C]_{tot} + [P]_{tot} + K_d \right) - \sqrt{\left([C]_{tot} + [P]_{tot} + K_d \right)^2 - 4[C]_{tot}[P]_{tot}} \right] \quad (2)$$

In this relationship, r_0 and r are the anisotropies of FtsZ-bound BoGTPγS in the absence and presence of compound, respectively; r_∞ is the anisotropy of FtsZ-bound BoGTPγS in the presence of an infinite compound concentration; and $[C]_{tot}$ and $[P]_{tot}$ are the total concentrations of compound and protein, respectively.

2.3. FtsZ GTPase assay

The impact of TXY436 on the GTPase activity of *E. coli* FtsZ was assayed by measuring the inorganic phosphate (P_i) released upon GTP hydrolysis by FtsZ in the absence or presence of compound via an end-point malachite green colorimetric assay. This assay is based on the spectrophotometric detection of the green complex formed between malachite green molybdate and P_i under acidic conditions. Triplicate reactions of 20 μL were assembled in half-volume, flat-bottom, 96-well microtiter plates containing 10 μM FtsZ and TXY436 (at concentrations ranging from 0 to 240 μM) in buffer containing 50 mM Tris-HCl (pH 7.4), 50 mM KCl, 10 mM magnesium acetate, and 10 mM $CaCl_2$. The reactions were pre-equilibrated for 10 min at room temperature, whereupon the GTPase activity was then initiated by the addition of 1 mM GTP and shifting the plates to 37 °C. The GTPase reactions were allowed to proceed for 2 h, and terminated by the addition of 80 μL of a malachite green reagent, which had been previously prepared by mixing a solution of 0.045% (w/v) malachite green (made in water) with a solution of 4.2% (w/v) ammonium molybdate (made in 4 M HCl) at ratio of 3 to 1, and filtering through a 0.22-μm filter. After addition of the malachite green reagent to the 96-well plates (which diluted the concentration of P_i in each well by 5-fold), the plates were incubated at room temperature for 1 min, and the absorbance at 620 nm was recorded using a VersaMax plate reader. The concentration of P_i released in each reaction was determined by using a phosphate standard curve, which was obtained by diluting a 200 μM KH_2PO_4 stock solution to achieve final phosphate concentrations ranging from 0 to 30 μM. The P_i released in the presence of each compound is reported as a percentage of P_i released in the absence of compound (*i.e.*, in the presence of DMSO vehicle alone).

2.4. FtsZ polymerization assay

Polymerization of *E. coli* FtsZ was monitored using a microtiter plate-based spectrophotometric assay in which changes in FtsZ polymerization are reflected by corresponding changes in absorbance at 340 nm (A_{340}). DMSO vehicle, TXY436 (at concentrations ranging from 0 to 30 μg/mL) or ampicillin (at a concentration of 30 μg/mL) was combined with 10 μM FtsZ in 100 μL of reaction

solution, which contained 50 mM Tris-HCl (pH 7.4), 50 mM KCl, 10 mM magnesium acetate, and 10 mM $CaCl_2$. Reactions were assembled in half-volume, flat-bottom, 96-well microtiter plates, and initiated by addition of 4 mM GTP. Polymerization was continuously monitored at 25 °C by measuring A_{340} in a VersaMax plate reader over a time period of 3 h.

2.5. Minimum inhibitory concentration (MIC) assays

MIC assays were conducted in accordance with Clinical and Laboratory Standards Institute (CLSI) guidelines for broth microdilution [31]. Briefly, log-phase *E. coli*, *K. pneumoniae*, or *A. baumannii* bacteria were added to 96-well microtiter plates (at 5×10^5 colony forming units [CFU]/mL) containing two-fold serial dilutions of compound or comparator drug (minocycline) in cation-adjusted Mueller-Hinton (CAMH) broth (Becton, Dickinson and Co., Franklin Lakes, NJ). Compound and drug concentrations (each concentration being present in duplicate) ranged from 64 to 0.031 μg/mL in all assays. The final volume in each well was 0.1 mL, and the microtiter plates were incubated aerobically for 24 h at 37 °C. Bacterial growth was then monitored by measuring OD_{600} using a VersaMax plate reader (Molecular Devices, Inc., Sunnyvale, CA), with the MIC being defined as the lowest compound concentration at which growth was ≥90% inhibited compared to antibiotic-free control. The following bacterial strains were included in these assays: *E. coli* strains W4573, N43 (*acrA1*), LZ2301 (*ΔmdfA*), LZ2096 (*ΔnorE*), LZ2310 (*acrA1 mdfA ΔnorE*) and ATCC BAA201 (an extended spectrum β-lactamase [ESBL]-producing strain that expresses the TEM-3 β-lactamase), *K. pneumoniae* ATCC 13883, and *A. baumannii* ATCC 19606. When present, PAβN was used at a concentration of 100 μg/mL in the *E. coli* experiments and 200 μg/mL in the *K. pneumoniae* and *A. baumannii* experiments.

2.6. Minimum bactericidal concentration (MBC) assays

MBC assays were conducted in accordance with CLSI guidelines [31]. Broth microdilution assays were conducted as described in the preceding section. After the 24-h incubation period, the number of survivors in wells that exhibited no growth was determined by plating on to tryptic soy agar (TSA) (Becton, Dickinson and Co., Franklin Lakes, NJ). The colonies that grew on the TSA plates after 24 h of incubation at 37 °C were counted, with MBC being defined as the lowest compound concentration resulting in a ≥3-log reduction in the number of colony forming units (CFUs).

2.7. Phase contrast microscopy

Log-phase *E. coli* W4573 or *K. pneumoniae* ATCC 13883 cells were cultured in CAMH broth at 37 °C for 4 h in the presence of PAβN (100 μg/mL for *E. coli* and 200 μg/mL for *K. pneumoniae*) and either DMSO (solvent control), 2× MIC of TXY436 (16.0 μg/mL for both *E. coli* and *K. pneumoniae*), or 2× MIC of minocycline (0.25 μg/mL for *E. coli* and 0.125 μg/mL for *K. pneumoniae*). A 1 mL sample was withdrawn from each bacterial culture, and centrifuged at 16,000*g* for 3 min at room temperature. The supernatant was then removed and the bacterial pellet was washed with 1 mL of phosphate-buffered saline (PBS) (Lonza Group Ltd., Walkersville, MD). The final bacterial pellet was then resuspended in 50 μL of PBS, with 5 μL of the resulting bacterial suspension being transferred onto a microscope slide together with 5 μL of 1% molten agarose (made in PBS). A cover slip was then applied and the slide was visualized with a Zeiss Axioplan 2 microscope equipped with a Plan-Apochromat 100× objective (NA = 1.40). Images were captured with a Zeiss Axiocam HR camera using the OpenLab software package.

2.8. Fluorescence microscopy

The impact of TXY436 on FtsZ Z-ring formation in *E. coli* KG22 bacteria was assessed in a manner similar to that described previously for berberine [29]. Specifically, exponentially growing KG22 bacteria were cultured in CAMH broth containing 100 μg/mL PAβN for 30 min at 37 °C in the presence of DMSO (solvent control) or 16 μg/mL TXY436. Expression of YFP-conjugated FtsZ was then induced by addition of L-arabinose to a final concentration of 0.2% (w/v), and the cells were incubated for 1 additional hour at 37 °C. The expression of YFP-conjugated FtsZ was then arrested by addition glucose to a final concentration of 0.2% (w/v), and the cells were incubated for an additional 30 min at 37 °C. The bacterial cultures were then treated and visualized as described above, with the additional incorporation of a standard GFP filter set.

3. Results

3.1. The presence of the conversion product of TXY436 (PC190723) alters the fluorescence anisotropy of BoGTPγS bound to E. coli FtsZ in a manner that is inconsistent with displacement of the bound nucleotide from the protein.

We have previously shown that the anisotropy of BoGTPγS (a fluorescent non-hydrolyzable GTP analog) bound to FtsZ can be altered by compounds that interact with the protein [17]. We sought to determine the impact, if any, of the presence of PC190723 (the conversion product of TXY436) on the anisotropy of BoGTPγS bound to purified *E. coli* FtsZ *in vitro*. To this end, the anisotropy of *E. coli* FtsZ-bound BoGTPγS was recorded in the presence of increasing concentrations of PC190723 and compared with the corresponding anisotropy of unbound (FtsZ-free) BoGTPγS, with the results being shown in Fig. 2A. For comparative purposes, unlabeled non-fluorescent GTP was included as a control in these assays. Upon binding to *E. coli* FtsZ, the anisotropy of BoGTPγS increases by approximately six-fold. Addition of increasing concentrations of unlabeled GTP induces a marked decrease in the anisotropy of FtsZ-bound BoGTPγS to a level equivalent to that associated with unbound BoGTPγS. This observation is consistent with the induced release of FtsZ-bound BoGTPγS that would be expected to result from the addition of an excess of unlabeled GTP relative to BoGTPγS. A comparison of the anisotropy profile for GTP addition with the corresponding profile for PC190723 addition reveals two key features:

(i) The addition of increasing concentrations of PC190723 also results in a decrease in the anisotropy of FtsZ-bound BoGTPγS. This PC190723-induced reduction in BoGTPγS anisotropy is indicative of a binding reaction with the *E. coli* FtsZ protein.
(ii) The extent to which the addition of PC190723 reduces the anisotropy of FtsZ-bound BoGTPγS is significantly less than that associated with the addition of GTP, and does not approach the anisotropy of unbound BoGTPγS, even at a 240-fold excess of PC190723 (240 μm) relative to BoGTPγS (1 μM). These findings suggest that the binding of PC190723 to *E. coli* FtsZ is not associated with the release of bound GTP and, therefore, also imply that the compound does not target the nucleotide binding pocket of the protein.

Recent crystallographic studies have demonstrated that PC190723 targets a specific site on *S. aureus* FtsZ that is distal from the GTP binding pocket [32,33]. Given this important structural information, we conducted additional anisotropy studies with *S. aureus* FtsZ similar to those described above for

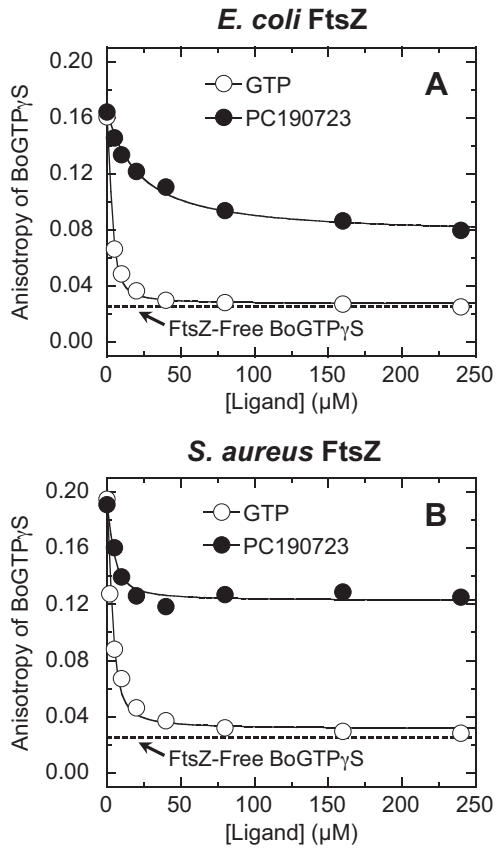

Fig. 2. Fluorescence anisotropies of *E. coli* FtsZ-bound (A) and *S. aureus* FtsZ-bound (B) BoGTPγS (1 μM BoGTPγS, 5 μM FtsZ) as a function of increasing concentrations of non-fluorescent unlabeled GTP (○) or PC190723 (●). The dashed lines represent the anisotropy value of 1 μM BoGTPγS in the absence of FtsZ (FtsZ-free BoGTPγS). The solid lines reflect the nonlinear least squares fits of the data with Eq. (2).

E. coli FtsZ, with the results of these additional studies being shown in Fig. 2B. Significantly, the anisotropy behavior pattern in the presence of added PC190723 and GTP was similar for both FtsZ proteins (compare Fig. 2A and B). This concordance suggests that the site on *E. coli* FtsZ targeted by PC190723 may be similar to the corresponding site it targets on *S. aureus* FtsZ.

3.2. TXY436 exerts little or no impact on the GTPase activity of E. coli FtsZ

The anisotropy results described above are consistent with the PC190723 conversion product of TXY436 targeting a site on *E. coli* FtsZ distinct from the GTP binding pocket. As such, TXY436 would not be expected to inhibit the GTPase activity of *E. coli* FtsZ to any significant degree. We probed for this behavior using TXY436 concentrations ranging from 1 to 240 μM. As the half-life for the conversion of TXY436 to PC190723 at the assay pH of 7.4 is approximately 18 min [27], the 2-h reaction time used in these GTPase determinations was sufficient for the near complete conversion of TXY436 to its PC190723 product. Our results revealed that the presence of TXY436 did not significantly impact the GTPase activity of *E. coli* FtsZ, with the GTPase activity at the highest compound concentration (240 μM) being almost identical to the GTPase activity in the absence of compound (not shown). Thus, the GTPase results are consistent with the BoGTPγS anisotropy results described above in implying that the PC190723 conversion product of TXY436 targets a site on *E. coli* FtsZ distinct from the GTP binding pocket of the protein.

Table 1
Affinities of PC190723 and GTP for *E. coli* and *S. aureus* FtsZ[a].

Compound	K_d (μM)	
	E. coli FtsZ	*S. aureus* FtsZ
PC190723	18.9 ± 2.3	2.2 ± 0.8
GTP	0.8 ± 0.1	1.0 ± 0.3

[a] K_d values were derived from the fits of the data shown in Fig. 2 with Eq. (2). The indicated uncertainties reflect the standard deviations of the experimental data from the fitted curves.

3.3. The PC190723 conversion product of TXY436 binds to E. coli FtsZ with an approximately nine-fold lower affinity than to S. aureus FtsZ.

We next sought to compare the affinities of the PC190723 conversion product of TXY436 for *E. coli* and *S. aureus* FtsZ. To this end, we analyzed the PC190723-induced reductions in BoGTPγS anisotropy shown in Fig. 2A and B with Eq. (2) to yield compound-protein dissociation constants (K_d). For comparative purposes, we also analyzed the corresponding GTP-induced reductions in BoGTPγS anisotropy. Note that the 1:1 binding formalism on which Eq. (2) is predicated yields excellent fits ($R^2 > 0.98$) of all the anisotropy profiles (the solid lines in Fig. 2A and B). The K_d values obtained from these fits are listed in Table 1. Inspection of these data reveals that PC190723 binds to *E. coli* FtsZ (K_d = 18.9 ± 2.3 μM) with an approximately nine-fold lower affinity than to *S. aureus* FtsZ (K_d = 2.2 ± 0.8 μM). By contrast, GTP binds to the two FtsZ proteins with a similar affinity (K_d = 0.8 ± 0.1 μM for *E. coli* FtsZ and K_d = 1.0 ± 0.3 μM for *S. aureus* FtsZ).

3.4. TXY436 inhibits the polymerization of E. coli FtsZ in a concentration dependent manner

We have previously shown that TXY436 stimulates the polymerization of purified *S. aureus* FtsZ [27]. We next sought to examine whether the presence of TXY436 impacts the polymerization activity of *E. coli* FtsZ. To assay this FtsZ function, we utilized a microtiter plate-based spectrophotometric assay in which FtsZ polymerization and bundling is detected in solution by a time-dependent increase in solution absorbance at 340 nm (A_{340}). Fig. 3 show the time-dependent A_{340} profiles of *E. coli* FtsZ in the presence of TXY436 at concentrations ranging from 0 to 30 μg/mL. Note that the presence of TXY436 decreases the extent of *E. coli* FtsZ polymerization/bundling, with the magnitude of these inhibitory effects increasing with increasing compound concentration. Thus, in marked contrast to its stimulatory effect on *S. aureus* FtsZ polymerization *in vitro* [27], the presence of TXY436 appears to inhibit the polymerization and/or bundling of *E. coli* FtsZ.

3.5. TXY436 is intrinsically inactive against E. coli, except upon genetic inactivation of the AcrAB efflux pump

We assessed the antibacterial activity of TXY436 versus four different efflux pump mutant strains of *E. coli* (N43, LZ2301, LZ2096, and LZ2310) as well as their wild-type homolog strain (W4573). Strains N43, LZ2301, and LZ2096 have inactivating mutations in the AcrAB, MdfA, and NorE efflux pumps, respectively. Strain LZ2310 has inactivating mutations in all three efflux pumps. TXY436 was essentially inactive against all the bacterial strains (with MIC values >64 μg/mL), except for single mutant strain N43 and the triple mutant strain LZ2310, against which the compound was associated with an MIC of 8.0 μg/mL (Table 2). The >16-fold enhanced potency of TXY436 versus N43 and LZ2310 relative to W4573, LZ2301, and LZ2096 indicates that the PC190723 conversion product of TXY436 is a substrate of the

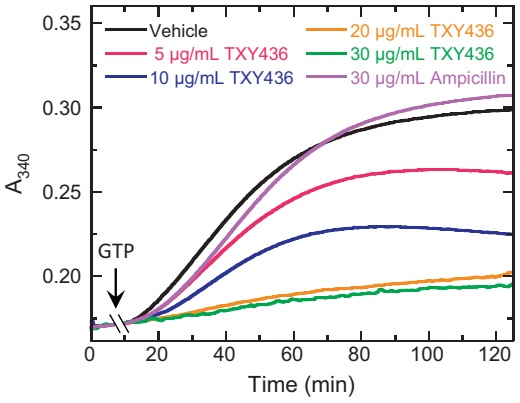

Fig. 3. Concentration dependence of the impact of TXY436 on the polymerization of *E. coli* FtsZ, as determined by monitoring time-dependent changes in absorbance at 340 nm (A_{340}) at 25 °C. The time-dependent A_{340} polymerization profiles were acquired in the presence of vehicle (DMSO) control or the indicated concentrations of TXY436 (ranging from 5 to 30 μg/mL). The polymerization profile acquired in the presence of ampicillin at 30 μg/mL is also included as a negative (non-FtsZ-targeting) control. Polymerization reactions were initiated by the addition of 4 mM GTP at the time indicated by the arrow.

Table 2
Activity of TXY436 against wild-type (WT) and efflux pump mutant strains of *E. coli*.

Strain	MIC (μg/mL)	
	TXY436	Minocycline[a]
WT (W4573)	>64	2.0
acrA1 (N43)	8.0	0.25
Δ*mdfA* (LZ2301)	>64	2.0
Δ*norE* (LZ2096)	>64	2.0
Δ*mdfA* Δ*norE acrA1* (LZ2310)	8.0	0.25

[a] Minocycline is included as a comparator control antibiotic that is a known substrate of RND-type efflux pumps [34].

AcrAB efflux pump in *E. coli*. By contrast, it does not appear to be a substrate of either the MdfA or NorE efflux pump.

3.6. The efflux pump inhibitor PAβN confers TXY436 with activity not only against E. coli, but also against K. pneumoniae and A. baumannii

We next assessed the antibacterial activity of TXY436 versus a number of other different Gram-negative bacteria strains, including an ESBL-producing *E. coli* strain (ATCC BAA201) that expresses the TEM-3 β-lactamase, a *K. pneumoniae* strain (ATCC 13883), and an *A. baumannii* strain (ATCC 19606). As was the case against *E. coli* W4573, TXY436 was essentially inactive against all the other bacterial strains examined (with MIC values >64 μg/mL) (Table 3). To determine whether the PC190723 product of TXY436 might be serving as a substrate of RND-type efflux pumps like AcrAB in these bacterial strains, we evaluated the impact of the RND-type efflux pump inhibitor PAβN [34] on the activity TXY436. Significantly, the presence of sub-inhibitory concentrations of PAβN conferred TXY436 with activity against all the bacterial strains (MIC = 8.0 μg/mL versus *E. coli* [including the ESBL-producing strain], 8.0 μg/mL versus *K. pneumoniae*, and 16 μg/mL versus *A. baumannii*) (Table 3). Thus, the PC190723 conversion product of TXY436 serves as a substrate of RND-type efflux pumps not only in *E. coli*, but also in *K. pneumoniae* and *A. baumannii*. The activity of minocycline (used as a control antibiotic that is a known substrate of RND-type efflux pumps [35]) was predictably enhanced by the presence of PAβN against all the efflux pump-expressing bacterial strains examined (Table 3).

Table 3
Impact of the efflux pump inhibitor PAβN on the activity of TXY436 against various Gram-negative bacteria.

Strain	MIC (μg/mL)			
	TXY436		Minocycline	
	− PAβN	+ PAβN	− PAβN	+ PAβN
E. coli W4573	>64	8.0	2.0	0.25
E. coli ATCC BAA201[a]	>64	8.0	32	0.5
K. pneumoniae ATCC 13883	>64	8.0	0.5	0.063
A. baumannii ATCC 19606	>64	16	0.13	0.031

[a] ATCC BAA201 is an ESBL-producing strain of *E. coli* that expresses the TEM-3 β-lactamase.

3.7. In the presence of PAβN, the activity of TXY436 against E. coli and K. pneumoniae is bactericidal in nature

We next examined whether the observed antibacterial activity of TXY436 in the presence of PAβN is bactericidal or bacteriostatic in nature. To this end, the MBC values of TXY436 against two *E. coli* strains (W4573 and ESBL-producing ATCC BAA201) and one *K. pneumoniae* strain (ATCC 13883) were determined and subsequently compared with the corresponding MIC values against these bacteria. In the presence of PAβN, the MBC value for TXY436 against each of the three strains examined was 16 μg/mL. A comparison of these MBC values with the corresponding MIC values listed in Table 3 yields an MBC/MIC ratio of 2 for all three strains. As per CLSI guidelines [31], such a ratio is indicative of a bactericidal mode of action. Thus, the activity of TXY436 against Gram-negative bacteria appears bactericidal in nature, a behavior analogous to its bactericidal activity against Gram-positive bacteria (*e.g.*, *S. aureus*) [27].

3.8. In the presence of PAβN, TXY436 induces changes in the morphology of E. coli and K. pneumoniae consistent with inhibition of cell division

The studies described above have indicated that TXY436 (through its conversion product PC190723) is able to target purified *E. coli* FtsZ *in vitro* and is active against *E. coli* and two other Gram-negative bacteria (*K. pneumoniae* and *A. baumannii*) when RND-type efflux pump activity is genetically or chemically inhibited. We next sought to determine if the bactericidal activity of TXY436 against *E. coli* and *K. pneumoniae* whose RND-type efflux pump activity has been inhibited with PAβN is the result of disrupted cell division and FtsZ function. One of the hallmarks of FtsZ-targeting compounds that disrupt bacterial cell division is the induction of an enlarged phenotype, which, in the case of rod-shaped bacteria, takes the form of a filamentous morphology [10,12,13,23,27,32]. Our first step was therefore directed toward examining the impact of TXY436 treatment on the morphology of *E. coli* and *K. pneumoniae* co-treated with PAβN. Co-treatment with PAβN and DMSO resulted in *E. coli* and *K. pneumoniae* bacteria with an average length of ~1 μm (Fig. 4A and D), as expected for these bacteria. By contrast, co-treatment with PAβN and TXY436 resulted in bacteria that were significantly more filamentous, with average lengths ranging from approximately 18 to 34 μm (Fig. 4B and E). Thus, TXY436 was able to induce the type of filamentous morphological change in PAβN-co-treated *E. coli* and *K. pneumoniae* that is a hallmark of FtsZ-directed inhibitors of cell division in rod-shaped bacteria [10,12,13,23,27,32]. Minocycline was used as a non-FtsZ-targeting control agent that is also a substrate of RND-type efflux pumps [35]. As expected, minocycline treatment did not impact the morphology of the bacteria to any significant degree (Fig. 4C and F).

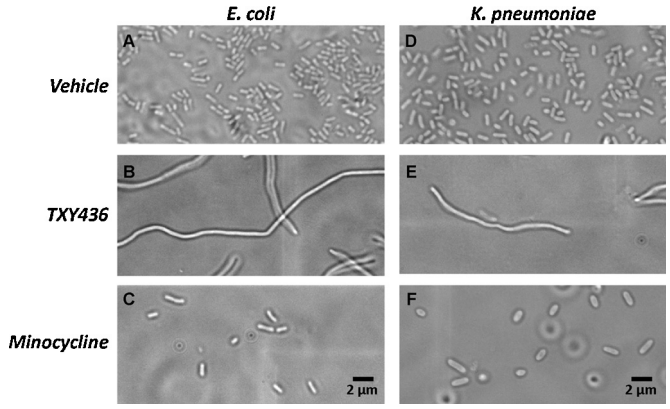

Fig. 4. Phase contrast micrographs of *E. coli* W4573 (A–C) and *K. pneumoniae* ATCC 13883 (D–F) bacteria cultured for 4 h in the presence of PAβN (100 μg/mL for *E. coli* and 200 μg/mL for *K. pneumoniae*) and either vehicle (DMSO) control (A and C), 2× MIC of TXY436 (16.0 μg/mL for both *E. coli* and *K. pneumoniae*) (B and E), or 2× MIC of minocycline (0.25 μg/mL for *E. coli* and 0.125 μg/mL for *K. pneumoniae*) (C and F).

3.9. In the presence of PAβN, TXY436 inhibits the formation of functional FtsZ Z-rings in E. coli

We next examined the impact of TXY436 on FtsZ function in *E. coli*. To this end, we monitored the impact of the compound on the formation of functional FtsZ Z-rings using a strain of *E. coli* (KG22-pLAU80) that inducibly expresses YFP-tagged FtsZ [29]. We co-treated KG22-pLAU80 bacteria with PAβN and either DMSO (vehicle control) or TXY436 and examined the bacteria using fluorescence microscopy. Vehicle-treated bacteria were of normal size and exhibited fluorescent foci corresponding to Z-rings (Fig. 5A). Some of the vehicle-treated bacterial cells had more than one apparent Z-ring, a behavior that may be due to the effects of FtsZ overexpression in the bacteria. Such behavior has been reported previously for the KG22-pLAU80 bacteria [29]. In contrast to vehicle-treated bacteria, TXY436-treated bacteria were filamentous in nature, with many exhibiting no fluorescent foci, but rather diffuse fluorescence distributed throughout the elongated cell (Fig. 5B). Some of the filamentous bacteria that result from TXY436 treatment exhibited multiple fluorescent foci (one such bacterial cell is highlighted by the arrow in Fig. 5B). It is not clear whether these foci reflect mature Z-rings or other FtsZ polymeric structures. In either case, the filamentous phenotype of the bacteria indicates that the FtsZ structures reflected by the fluorescent foci are not functionally competent for cell division.

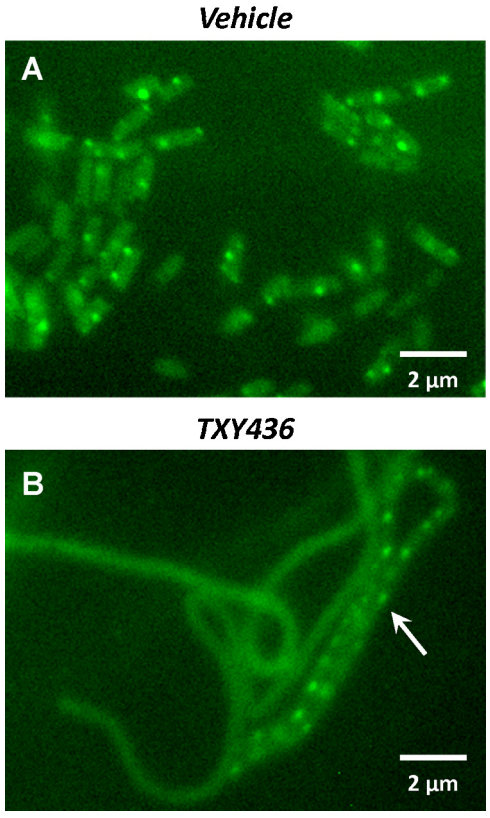

Fig. 5. Fluorescence micrographs of *E. coli* KG22-pALU80 bacteria (which express YFP-tagged FtsZ) in the presence of 100 μg/mL PAβN and either vehicle (DMSO) control (A) or 16 μg/mL TXY436 (B). The arrow in panel (B) highlights a TXY436-treated bacterial cell that exhibits multiple fluorescent foci.

4. Discussion

The FtsZ-targeting agent PC190723 and related benzamide compounds are associated with potent activity against Gram-positive staphylococci and bacilli [13,23,25,27,36]. However, they exhibit poor intrinsic activity against Gram-negative bacteria [13,23,36]. One possible explanation for the inactivity of PC190723 against *E. coli* is an inability of the compound to target *E. coli* FtsZ [26]. Our fluorescence anisotropy results with purified *E. coli* FtsZ *in vitro* indicate that PC190723 (the conversion product of TXY436) can indeed bind to the protein in a manner that alters the anisotropy of FtsZ-bound GTPγS (Fig. 2A). The PC190723 binding site on *E. coli* FtsZ appears to be distinct from the GTP binding pocket, as the magnitude of the PC190723-induced alteration in GTPγS anisotropy is substantively less than that caused by the binding of unlabeled non-fluorescent GTP (Fig. 2A). The minimal impact of PC190723 on the GTPase activity of *E. coli* FtsZ also lends support to this conclusion. We suggest that the change in GTPγS anisotropy induced by PC190723 binding reflects an induced conformational change in the FtsZ protein that alters the structure of the GTP binding pocket in a manner that impacts the anisotropy properties of the bound nucleotide analog. Such a conformational change could also result in an altered propensity for the *E. coli* FtsZ protein to polymerize and/or to form polymeric bundles. In this connection, the results of our polymerization studies indicate that PC190723 does in fact reduce the propensity for *E. coli* FtsZ polymerization and bundling in a manner dependent on compound concentration (Fig. 3).

A comparison of PC190723 binding to *E. coli* FtsZ relative to *S. aureus* FtsZ revealed a similar overall impact on the anisotropy of bound GTPγS (Fig. 2). The crystal structure of PC190723 in complex with *S. aureus* FtsZ has been recently reported [32,33]. In this structure, PC190723 targets a site distal from the GTP binding pocket and centered about residues G196 and N263, which, when mutated, induce staphylococcal resistance to the compound [13]. It is possible that PC190723 may target the corresponding site in *E. coli* FtsZ, although our analysis of the GTPγS anisotropy data (Fig. 2) reveals that the compound targets the *E. coli* FtsZ site with an approximately nine-fold lower affinity than it does the *S. aureus* FtsZ site (Table 1).

The ability of the PC190723 conversion product of TXY436 to target *E. coli* FtsZ *in vitro* raised the question as to why PC190723 is intrinsically inactive against *E. coli*, and, for that matter, other Gram-negative bacteria. We hypothesized that the inactivity of PC190723 versus Gram-negative bacteria may be due, at least in part, to the compound being a substrate of efflux pumps that are expressed in these bacteria. Our antibacterial results support this hypothesis. Specifically, our results indicate that genetic or chemical inactivation of RND-type efflux pumps (*e.g.*, AcrAB) confers PC190723 with activity against the Gram-negative

pathogens *E. coli*, *K. pneumoniae*, and *A. baumannii* (Tables 2 and 3). By contrast, genetic inactivation of major facilitator (MF)- and multidrug and toxic compound extrusion (MATE)-type efflux pumps (*e.g.*, MdfA and NorE, respectively) does not appear to impact PC190723 activity (Table 2). Although RND-type efflux pump inactivation confers PC190723 with activity against *E. coli*, *K. pneumoniae*, and *A. baumannii*, the magnitude of that activity is 8- to 16-fold lower than that previously reported for the compound against *S. aureus* [13,23,25,27,36]. With regard to *E. coli*, this differential activity may reflect, at least in part, the reduced affinity of PC190723 for *E. coli* relative to *S. aureus* FtsZ (Table 1).

While our *in vitro* results indicate that the PC190723 conversion product of TXY436 is able to target purified *E. coli* FtsZ, they do not necessarily imply that the compound is targeting FtsZ in bacteria. We therefore sought to determine whether the activity of PC190723 we observed upon RND-type efflux pump inactivation in *E. coli*, *K. pneumoniae*, and *A. baumannii* correlated with the disruption of cell division and FtsZ function. The pronounced filamentous morphology induced in *E. coli* and *K. pneumoniae* upon co-treatment with PAβN and TXY436 (Fig. 4) is consistent with the disruption of cell division by the compound. Furthermore, our fluorescence microscopy studies using a strain of *E. coli* (KG22-pLAU80) that expresses YFP-tagged FtsZ suggested that co-treatment with PAβN and TXY436 disrupted ability of the bacterial cell to form functional Z-rings (Fig. 5). Recently, Fenton and Gerdes [37] reported a similar behavior in *E. coli* in which an interaction between the essential cell division protein MreB and FtsZ was abrogated due to a mutation in MreB. They showed that this interaction could be restored through mutations in specific FtsZ residues [37]. Interestingly, the FtsZ residues they identified as being important for FtsZ interaction with MreB border the target binding site on *E. coli* FtsZ we are invoking for PC190723, namely, the site corresponding to that revealed by the recently reported crystallographic studies of the PC190723-*S. aureus* FtsZ complex [32,33]. It is therefore possible that PC190723 binding to *E. coli* FtsZ may disrupt the FtsZ interaction with MreB and thereby interfere with cell division. Future studies will be directed toward assessing the veracity of this hypothesis.

In the aggregate, our results suggest that the intrinsic inactivity of PC190723 against the Gram-negative bacteria *E. coli*, *K. pneumoniae*, and *A. baumannii* is due to the actions of RND-type efflux pumps in these bacteria rather than to an inability of the compound to target the FtsZ proteins of the bacteria. Even with efflux pump inactivation, the MICs we observe against Gram-negative bacteria are $\geq$8 μg/mL. For clinical utility, lower MICs would be more desirable. Thus, future efforts will be directed toward the development of next-generation analogs with increased FtsZ affinity and enhanced antibacterial potency when combined with an EPI.

Conflict of interest

Drs. Daniel S. Pilch and Edmond J. LaVoie are co-founders of TAXIS Pharmaceuticals, Inc. and therefore have a financial interest in the company.

Acknowledgments

This study was supported by research agreements between TAXIS Pharmaceuticals, Inc. and both Rutgers Robert Wood Johnson Medical School (D.S.P) and Rutgers Ernest Mario School of Pharmacy (E.J.L.). We are indebted to Dr. Lynn Zechiedrich (Baylor College of Medicine, Houston, TX) for providing us with the *E. coli* W4573, N43 (*acrA1*), LZ2301 (*ΔmdfA*), LZ2096 (*norE*), and LZ2310 (*acrA1 ΔmdfA ΔnorE*) strains. We are also indebted to Dr. Liam Good (Royal Veterinary College, University of London, England) for providing us with the *E. coli* KG22-pLAU80 strain.

References

[1] Bi EF, Lutkenhaus J. FtsZ ring structure associated with division in *Escherichia coli*. Nature 1991;354:161–4.
[2] Addinall SG, Bi E, Lutkenhaus J. FtsZ ring formation in *fts* mutants. J Bacteriol 1996;178:3877–84.
[3] Dai K, Lutkenhaus J. FtsZ is an essential cell division gene in *Escherichia coli*. J Bacteriol 1991;173:3500–6.
[4] Adams DW, Errington J. Bacterial cell division: assembly, maintenance and disassembly of the Z ring. Nat Rev Microbiol 2009;7:642–53.
[5] Erickson HP, Anderson DE, Osawa M. FtsZ in bacterial cytokinesis: cytoskeleton and force generator all in one. Microbiol Mol Biol Rev 2010;74:504–28.
[6] Lutkenhaus J, Addinall SG. Bacterial cell division and the Z ring. Annu Rev Biochem 1997;66:93–116.
[7] Egan AJ, Vollmer W. The physiology of bacterial cell division. Ann N Y Acad Sci 2013;1277:8–28.
[8] Kirkpatrick CL, Viollier PH. New(s) to the (Z-) ring. Curr Opin Microbiol 2011;14:691–7.
[9] Lutkenhaus J, Pichoff S, Du S. Bacterial cytokinesis: from Z ring to divisome. Cytoskeleton 2012;69:778–90.
[10] Adams DW, Wu LJ, Czaplewski LG, Errington J. Multiple effects of benzamide antibiotics on FtsZ function. Mol Microbiol 2011;80:68–84.
[11] Awasthi D, Kumar K, Ojima I. Therapeutic potential of FtsZ inhibition: a patent perspective. Expert Opin Ther Pat 2011;21:657–79.
[12] Haydon DJ, Bennett JM, Brown D, Collins I, Galbraith G, Lancett P, et al. Creating an antibacterial with *in vivo* efficacy: synthesis and characterization of potent inhibitors of the bacterial cell division protein FtsZ with improved pharmaceutical properties. J Med Chem 2010;53:3927–36.
[13] Haydon DJ, Stokes NR, Ure R, Galbraith G, Bennett JM, Brown DR, et al. An inhibitor of FtsZ with potent and selective anti-staphylococcal activity. Science 2008;321:1673–5.
[14] Huang Q, Kirikae F, Kirikae T, Pepe A, Amin A, Respicio L, et al. Targeting FtsZ for antituberculosis drug discovery: noncytotoxic taxanes as novel antituberculosis agents. J Med Chem 2006;49:463–6.
[15] Huang Q, Tonge PJ, Slayden RA, Kirikae T, Ojima I. FtsZ: a novel target for tuberculosis drug discovery. Curr Top Med Chem 2007;7:527–43.
[16] Kapoor S, Panda D. Targeting FtsZ for antibacterial therapy: a promising avenue. Expert Opin Ther Targets 2009;13:1037–51.
[17] Kaul M, Parhi AK, Zhang Y, LaVoie EJ, Tuske S, Arnold E, et al. A bactericidal guanidinomethyl biaryl that alters the dynamics of bacterial FtsZ polymerization. J Med Chem 2012;55:10160–76.
[18] Kumar K, Awasthi D, Berger WT, Tonge PJ, Slayden RA, Ojima I. Discovery of anti-TB agents that target the cell-division protein FtsZ. Future Med Chem 2010;2:1305–23.
[19] Kumar K, Awasthi D, Lee SY, Zanardi I, Ruzsicska B, Knudson S, et al. Novel trisubstituted benzimidazoles, targeting *Mtb* FtsZ, as a new class of antitubercular agents. J Med Chem 2011;54:374–81.
[20] Lock RL, Harry EJ. Cell-division inhibitors new insights for future antibiotics. Nat Rev Drug Discovery 2008;7:324–38.
[21] Ma S. The development of FtsZ inhibitors as potential antibacterial agents. ChemMedChem 2012;7:1161–72.
[22] Schaffner-Barbero C, Martin-Fontecha M, Chacón P, Andreu JM. Targeting the assembly of bacterial cell division protein FtsZ with small molecules. ACS Chem Biol 2012;7:269–77.
[23] Stokes NR, Baker N, Bennett JM, Berry J, Collins I, Czaplewski LG, et al. An improved small-molecule inhibitor of FtsZ with superior in vitro potency, drug-like properties, and in vivo efficacy. Antimicrob Agents Chemother 2013;57:317–25.
[24] Anderson DE, Kim MB, Moore JT, O'Brien TE, Sorto NA, Grove CI, et al. Comparison of small molecule inhibitors of the bacterial cell division protein FtsZ and identification of a reliable cross-species inhibitor. ACS Chem Biol 2012;7:1918–28.
[25] Kaul M, Zhang Y, Parhi AK, Lavoie EJ, Tuske S, Arnold E, et al. Enterococcal and streptococcal resistance to PC190723 and related compounds: molecular insights from a FtsZ mutational analysis. Biochimie 2013;95:1880–7.
[26] Andreu JM, Schaffner-Barbero C, Huecas S, Alonso D, Lopez-Rodriguez ML, Ruiz-Avila LB, et al. The antibacterial cell division inhibitor PC190723 is an FtsZ polymer-stabilizing agent that induces filament assembly and condensation. J Biol Chem 2010;285:14239–46.
[27] Kaul M, Mark L, Zhang Y, Parhi AK, Lavoie EJ, Pilch DS. An FtsZ-targeting prodrug with oral antistaphylococcal efficacy *in vivo*. Antimicrob Agents Chemother 2013;57:5860–9.
[28] Yang S, Clayton SR, Zechiedrich EL. Relative contributions of the AcrAB, MdfA and NorE efflux pumps to quinolone resistance in *Escherichia coli*. J Antimicrob Chemother 2003;51:545–56.
[29] Boberek JM, Stach J, Good L. Genetic evidence for inhibition of bacterial division protein FtsZ by berberine. PLoS One 2010;5:e13745.
[30] Sorto NA, Olmstead MM, Shaw JT. Practical synthesis of PC190723, an inhibitor of the bacterial cell division protein FtsZ. J Org Chem 2010;75:7946–9.
[31] CLSI. Methods for dilution antimicrobial sucseptibility tests for bacteria that grow aerobically; approved standard. 8th ed. Wayne, PA: Clinical and Laboratory Standards Institute; 2009.

[32] Tan CM, Therien AG, Lu J, Lee SH, Caron A, Gill CJ, et al. Restoring methicillin-resistant *Staphylococcus aureus* susceptibility to β-lactam antibiotics. Sci Transl Med 2012;4:126ra135.
[33] Matsui T, Yamane J, Mogi N, Yamaguchi H, Takemoto H, Yao M, et al. Structural reorganization of the bacterial cell-division protein FtsZ from *Staphylococcus aureus*. Acta Crystallogr Sect D Biol Crystallogr 2012;D68:1175–88.
[34] Pagès JM, Masi M, Barbe J. Inhibitors of efflux pumps in Gram-negative bacteria. Trends Mol Med 2005;11:382–9.
[35] Murakami S, Nakashima R, Yamashita E, Matsumoto T, Yamaguchi A. Crystal structures of a multidrug transporter reveal a functionally rotating mechanism. Nature 2006;443:173–9.
[36] Stokes NR, Sievers J, Barker S, Bennett JM, Brown DR, Collins I, et al. Novel inhibitors of bacterial cytokinesis identified by a cell-based antibiotic screening assay. J Biol Chem 2005;280:39709–15.
[37] Fenton AK, Gerdes K. Direct interaction of FtsZ and MreB is required for septum synthesis and cell division in *Escherichia coli*. EMBO J 2013;32:1953–65.